Strojniški vestnik - Journal of Mechanical Engineering 68(2022)10, 623-634
DOI:10.5545/sv-jme.2022.169
Original Scientific Paper
Received for review: 2022-04-19
Received revised form: 2022-06-23
Accepted for publication: 2022-07-11

The Nickel Aluminide Coatings Obtained on Small Holes Produced with the EDD Method

Marcin Trajer[1,*] – Łukasz Pyclik[2] _ Jerzy Robert Sobiecki[1]

[1] Warsaw University of Technology, Faculty of Material Science and Engineering, Poland
[2] Silesian University of Technology, Faculty of Materials Engineering, Poland

Recently, airplane travel has become more affordable and thus more common. This has required engineers and scientists to spend thousands of hours on the development of new material and production technologies. High-pressure turbine (HPT) components are the most heavily loaded parts from the thermal, mechanical, and corrosion points of view. Therefore, both the material from which blades and vanes are cast as well as protective coatings are being constantly developed. Better material translates into longer and safer engine operation. Coatings maintain material structures within aggressive environments. However, despite the wide scope of development, there are areas that have not been investigated, one of which is electro-discharge drilling (EDD) machined cooling holes surface and its influence on environmental coating durability. In this paper, the EDD process impact on coating durability is shown. Process residuals, such as redeposited material and recast layers, result in coating inclusions. Oxidation testing also shows the relationship between the cooling hole diameter and coating durability.
Keywords: EDD method, nickel aluminide, turbine blade, durability, jet engine

Highlights

- *Continuous performance growth pushes the exhaust gases of jet engines to higher temperatures exceeding superalloys' melting temperatures.*
- *The most common (and the only commercially utilized) design method of HPT utilizes a cooling system that consists of cooling holes creating an insulating layer of cold air.*
- *Cooling holes are machined by means of non-conventional machining methods, which result in material melting, redeposition or evaporation. EDD is one such method.*
- *Parts durability was significantly improved with the environmental coating application; the most common are those based on Al with some modifications.*
- *Aggressive HPT environments affect the whole part. Most surfaces are coating-covered; however, cooling holes' surfaces are different than the cast surface of the airfoil. The hole surface is modified due to tge manufacturing process, which impacts chemistry, phase structure and roughness.*

0 INTRODUCTION

The growth of jet engines started in early 1940s [1] with their first application. Since then, each engine element has undergone significant development. Modern trends and requirements push component manufacturing to the technological limits. Advanced statistical methods, modelling, data mining, and neural networks are in use in the race. The goal is continuous product improvement in terms of weight, cost, and durability. At the same time, the thermodynamic basis used by Frank Whittle has not changed and remains in effect for the newest engines, such as GE9X or RR Trent7000. A more efficient thermal cycle translates into higher operation temperatures, reaching up to 1350 ºC to 1550 ºC of thermal barrier coating (TBC) temperature for recent commercial engines [2]. Therefore, more durable materials as well as new cooling methods [2] are needed. Advanced film cooling through micro holes or double wall castings allowing near-wall cooling are being investigated in parallel with more resistant environmental coatings [3]. An example of a modern highly cooled and TBC-covered high-pressure turbine (HPT) blade is shown in Fig. 1. Fig. 2 shows the relationship between component heat load, cooling effectiveness and new materials application.

Fig. 1. *Recent film-cooled high-pressure turbine blade covered with ceramic TBC coating [4]*

*Corr. Author's Address: Warsaw University of Technology, Faculty of Material Science and Engineering, Wołoska 141, 02-507 Warsaw, Poland marcin.trajer.dokt@pw.edu.pl

Improvements in high temperature creep and rupture properties contrast the machinability of those materials. In parallel with requirement for more sophisticated cooling systems and tighter tolerances [5], production methods are being studied for their enhancement. There are methods that might be used for cooling hole manufacturing. Li et al. [6] provide a comprehensive summary of the following drilling methods: mechanical, laser, electro-discharge, and electrochemical. Each method has its own advantages but also difficulties. Each method differently influences manufactured material surface properties including chemical and physical changes. Electro-discharge machining (EDM), laser, and chemical are contactless methods, but EDM and laser use heat, which influences surface integrity. In contrast, electro-chemical machining (ECM) of small holes relates to significant technological and environmental challenges. Mechanical drilling is an unsuitable technique for current heat-resistant alloys mainly due to technical issues related to material hardness and hole sizes (less than 1 mm in diameter). With the above short summary, there are two main techniques currently used for drilling and shaping holes cooling: electro-discharge drill (EDD) and laser. What is common for them is surface modification resulting from local melting and evaporation of the material. Melting can drive local changes in material chemical composition and crystallographic structure. As discussed by Zielinska [7], that can influence the environmental coating applied on such surfaces.

Numerous papers describe generic aspects of the EDD process, either from a general perspective, such as Kunieda et al. [8], or from a process parameters point of view, as presented by Machno [9]. Scientists look for optimal relationships between the material removal rate (MRR), surface roughness (SR) and tool wear (TW), as well as the post EDD surface condition and its susceptibility for fracturing [10]. Such studies allow for a better understanding of the process. That allows for its optimization by means of statistical and neural network analysis (NNA). Such models enable defining certain process parameters, which result in optimal process factors, such as MRR, TW, or SR.

The influence of EDD parameters on holes surface topography was verified by Novovic [11]. The impact on surface quality was studied by Ekmekci [12]. It was verified when certain parameters influence part life (roughness, cracks). However, even outstanding progress in cooling design and manufacturing is not enough to ensure the sufficient durability of the components. Fig. 3 shows a blade fracture example. That is mainly due to coatings being a limiting chain. For that reason, new protection methods are developed.

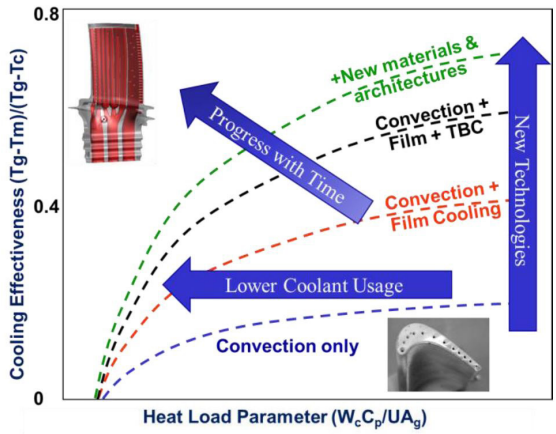

Fig. 2. *Notional component cooling technology curves* [2]

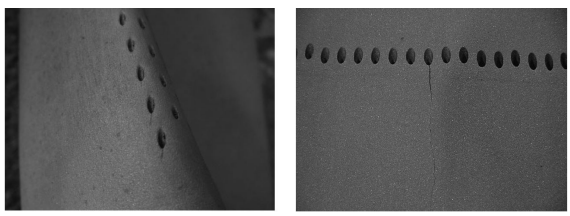

Fig. 3. *Examples of cracks initiated from EDD holes on rotating blades* [10]

Multiple studies have been performed regarding coating durability and methods for its improvement. Sun et al. showed the impact of cooling holes on part durability [13]. Accordingly, publications related to aluminide coating application, chemical composition and durability were reviewed, which revealed a lack of verification of whether the EDM manufacturing process had any impact on subsequently applied aluminide coating. This paper summarizes articles in which authors evaluated EDM cooling holes process as well as environmental aluminide coating durability. Additionally, initial tests verifying the interaction between aluminide coating and machined EDM surfaces is presented.

1 REVIEW OF EDD PROCESS AND ITS INFLUENCE ON SURFACE CONDITION

Within the electro-discharge drilling process, there is no tool material contact. No mechanical forces are applied by the tool. Material removal occurs due to energy transfer between the electrode and the part. Energy in the form of a spark causes local material melting and evaporation. Other models describe

that as a material disruption under thermal load. During operation, both the electrode and the part material are removed. Such process physics results in its complexity and specific surface conditions. The electro-discharge process has been under constant development and improvement since the 1940s when it was first developed. In 1943, Lazarenko and Lazarenko [14] investigated ways of preventing the erosion of tungsten electrical contacts due to sparking. They noticed that when the contacts were immersed in oil, sparking could result in controllable material removal. Simultaneously, a similar sparking tool for broken drill removal from aluminium castings was developed in the US. Over the years, several aspects of the EDM process have been evaluated.

One of the crucial factors of the EDD process is recast layer thickness and microcrack occurrence in the machined surfaces. Recast is a material that melted during sparking and then rapidly solidified see Fig. 4. Due to its cracking susceptibility, high hardness, and the number of microcracks, cracks and high tensile stress [15] recast layer thickness (RLT) reduction methods have been investigated. Li described with basic process parameters such as pulse width, pulse interval, voltage, current and flushing pressure within an experiment [16]. The study enabled an RLT reduction from 10.472 µm to 2.416 µm.

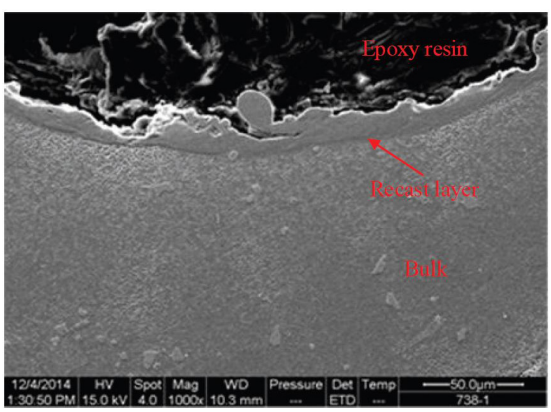

Fig. 4. *Recast layer picture by SEM* [15]

Swiercz et al. [17] shows key parameters impacting surface roughness as well as RLT. It was proved that key factor is pulse duration and current value. Similar, but not identical conclusions were shared by Lee [18]. The main factor responsible for RLT increase is pulse-on whereas current is listed as a second factor responsible for RLT thickness variation. Another key aspect of the EDM process used for small hole manufacturing is its accuracy. Process parameters influence not only surface roughness or its integrity but also manufacturing accuracy. Hole diameter and tapering are commonly evaluated parameters. Machno [9] shows that increases in pulse-on time reduces hole tapering. At the same time, the pulse current is indicated as the main contributor to increased hole taper [19].

However, even extremely durable turbine components equipped with advanced cooling systems are still exposed to exhaust gases in combustion products. Such an environment significantly influences material durability by oxidation and/ or corrosion. State-of-the art manufacturing itself is not capable of eliminating or even reducing that condition.

2 SURFACE PROTECTION

High operating temperature [20] negatively influences material mechanical properties, such as low cycle fatigue life, high cycle fatigue life, or creep. However, there are other factors with adverse effects. Corrosion and oxidation play significant roles in component degradation. Exhaust gases are rich in oxygen, and fuel combustion products have high sulphur context. Accompanied by high temperatures, these elements play a key role in material reduction [21].

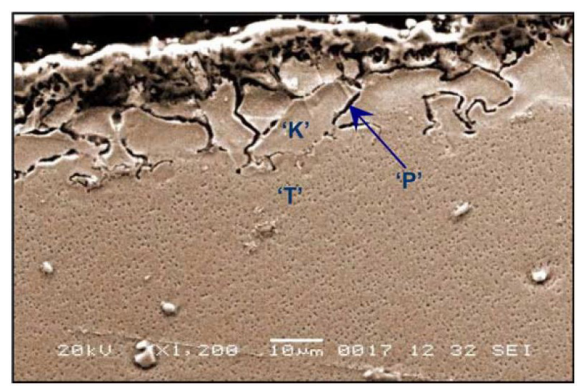

Fig. 5. *Corroded depleted zone (K)* [21]

Extensive research of protective coatings for nickel-based alloys started in the early 1960s [3]. Experiments proved that aluminide coatings provide the best environmental protection for nickel-based superalloys. Since then, aluminide coating technology has improved constantly. The most common verification method for new concepts is a cyclic oxidation test [22] and [23], which simulates engine-induced thermal and mechanical loads [3]. Such testing allows for material/coating oxidation resistance verification under transient thermal loads. Even verified as sufficient for the design, coating technology requires constant improvement. That

happens due to already mentioned situation: the technical race for more efficient jet engines and their longer flight times. As stated earlier, each new engine generation is designed for higher temperatures of its thermal cycle. That results in a larger spread of temperatures over turbine parts, especially nozzles. Improvements in coating system durability can be made in several ways. Historically, the first step was to improve the aluminide coating process to allow "self-healing" by alumina transfer. However, as the thermal gradient on the parts increases, coating brittleness becomes a significant issue. The search for improvement in that area led to different application methods **[24]** or specific dopants **[25]** to **[27]** such as rhodium, zirconium, hafnium, palladium, and yttrium. Another path is thermal gradient reduction, which reduces the spallation of the protective layer of alumina oxides. That is realized by the physical insulation of the metal surface from hot path gasses by ceramic coating. The application of those coatings, their properties and thermal loads resistance is another area of coatings, which is intensively investigated.

3 MATERIALS

Inconel 718 material samples were used; the plates had dimensions as follows: 50 mm × 25 mm × 3 mm. Table 1 shows material composition.

Table 1. *Inconel 718 composition*

	Ni	Cr	Nb	Mo	Ti
Inco 718	52.5	19	5.15	3.05	0.85
	Al	Co	Cu	C	Si/Mn
	0.5	1	0.3	0.08	0.35

Samples were cut from 3 mm thick sheet metal were delivered by TW Metals, Poland together with material certification.

Brass tube electrodes were used for EDD process. Material certification was not provided. SEM evaluation was performed to reveal material composition.

The SEM evaluation shows Cu/Zn composition at 70/30 rate (Fig. 6). This fits to ASTM B135 brass. This alloy is dedicated to extruded elements.

Within the EDD process, deionized water circulates in a closed system. Process debris are removed by two stage filtering system based on 5-micron paper filers. Constant 1 S/m water conductivity is maintained. If needed, ions are moved by resin source.

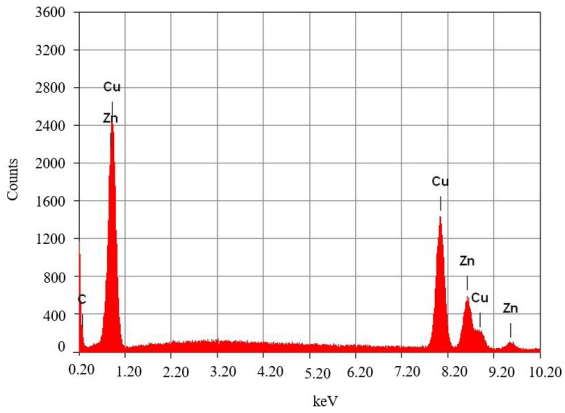

Element	keV	Mass [%]	Error [%]
Cu	8.04	68.67	1.53
Zn	8.63	31.33	1.96
Total		100	

Fig. 6. *Electrode material verification by means of EDS*

4 METHODS

4.1 Electro-Discharge Drilling

The drilled hole pattern is shown on Fig. 7. The smallest and medium holes were created by EDD, while the largest one was shaped by the electrode. Brass electrodes were used in all cases: 0.25 mm, 0.3 mm, and 0.3 mm milling, respectively. Holes are 30 deg inclined to the surface. Discharge parameters were identical between samples with the difference that largest holes were milled. That technique uses an electrode similarly to milling cutting tool. The electrode tip travels horizontally. All holes were drilled through and are open on both surfaces. Fig. 8 shows EDD system schematic.

Fig. 7. *Inconel 718 test samples*

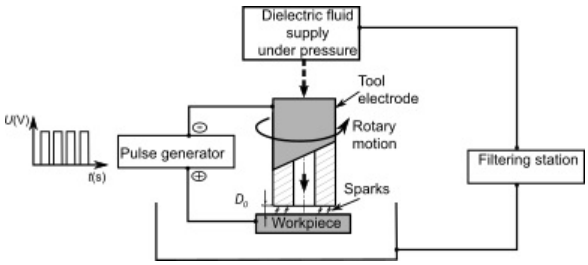

Fig. 8. *EDD system schematics*

4.2 Holes Geometrical Measurements

Pattern holes have been measured by means of an Alicona G5 optical system, which uses a variable focus method for surface scanning. A 10× lens dedicated for small holes inspection was used. After scanning, the data were transferred to the GOM Inspect software where measurements were done automatically with the macro-calculating best fit cylinder for each hole. Gaussian roughness distribution was used for inscribed cylinder fitting.

4.3 Out-of-pack Coating Process

Protective coating is frequently used in the aeronautics industry, especially on the blades of the high-pressure turbine, which run at very high temperatures and in a highly oxidizing atmosphere.

The out-of-pack or over-pack process operates in a manner like pack cementation except that the components to be coated are suspended either above the pack or below from the pack (vapour generator) retort.

The transfer of aluminium species from the vapour phase to the substrate occurs by gas-phase diffusion and by solid-phase diffusion of aluminium into the substrate to form the aluminide phases. The former increases the surface concentration of aluminium in the coating while the latter decreases it. The surface composition of the coating tends to reach a steady state value in a short time after the commencement of the process. In the vapour phase aluminizing, the rate of transport of aluminium to the substrate is much faster than the solid phase diffusion of aluminium into the substrate. Thus, the composition of aluminide coating is decided by the kinetics of the solid phase diffusion. The coating process is divided into several steps:

a) Formation of the aluminium subchlorides by the reaction of the aluminium metal or alloy and the aluminium chloride vapor;
b) Transport of the subchlorides to the substrate by gas-phase diffusion;
c) Reaction leading to the deposition of aluminium at the substrate surface;
d) Diffusion of aluminium into substrate with the formation of the coating consisting of different intermetallic phases;
e) Diffusion of the reaction products from the substrate back to the reactor.

Steps a) and c) are very fast at the operating temperature; therefore, the thickness of the coating process is controlled by step b) the vapor transport and d) the solid-phase diffusion. Step e) determines the purity of the coating [28].

The schematic diagram of the out-of-pack process is given in Fig. 9. The coating vapours are transported to the components by an inert carrier gas. The plumbing is designed so that the vapours can access both external and internal surfaces of the components. The retort is inserted into a furnace and held at the desired temperature for the selected duration.

This approach results in a much cleaner and uniform coating for very complicated geometry components, with no entrapped pack particles [28].

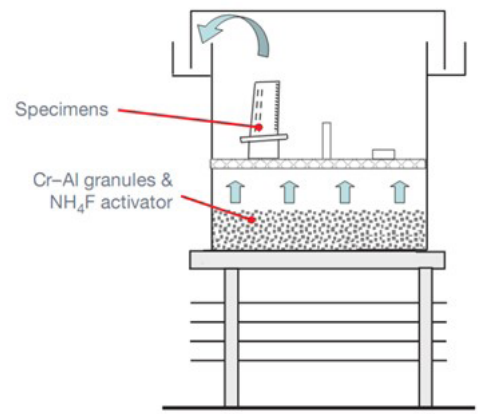

Fig. 9. *Schematic of the out-of-pack vapor phase aluminizing process*

4.4 Metallography and Coating Characterization

Analysis of the morphology, surface topography, and chemical composition of the coating was carried out by optical microscope. as well as by SEM equipped XRD evaluation and material composition. For visual observation, a Keyence VHX-7000 device was used. SEM evaluation was performed with a JEOL JSM-6490LA device equipped with an XRD extension.

The XRD phase composition of the obtained layers was determined with Brucker AXS D8

Discover diffractometer using CuK_α radiation with a wavelength of $\lambda = 0.154$ nm. In order to provide the opportunity to probe the structural evolution of solid near the surface, the grazing incidence X-ray diffraction (GIXRD) was used. A monochromatic X-ray beam with a wavelength of 0.15 nm was used. The GIXRD setup is equipped with a parabolic Göbel mirror and a conventional line focus Cu radiation tube (40 kV / 40 mA). The incidence angle was fixed at 2º with 2θ range 20º to 120º with step of 0.025º.

Adhesion of the coating to the Inconel substrate was verified using a CMS Instruments RST scratch tester with a diamond stylus with a 200 µm spherical tip radius. The indenter load was set to several values: 5 N, 20 N, 40 N, 60 N, 80 N, 100 N, and 200 N. All tests were performed over a 4 mm length. The adhesion of the coatings was evaluated based on an LC_3 curve. The LC_3 critical load occurs with the coating delamination force and was determined based on acoustic emission measured and post-test scratch images evaluation.

5 OXIDATION TESTING

Testing was performed in air atmosphere with a MAB FE37 furnace (Forno Mab, Italy) for oxidation testing. Samples were placed on ceramic support, heated in air up to 1100 ºC and treated for 23 hours. After that time, heating was turned off. Samples cooled down in the furnace.

5.1 Metallographic Evaluation

Metallurgical evaluation was performed with a Keyence VX7000 microscope. Keyence software was used.

6 EXPERIMENTAL PROCEDURE

6.1 Hole Manufacturing

Hole drilling was performed automatically using a CNC-coded procedure. All holes were drilled with same parameters. Moreover, each new electrode was checked for minimum water flow. If the flow rate was below a certain level, the electrode was assumed to be not acceptable and replaced with a new one. Samples were hold by dedicated fixture ensuring position repeatability. Manual assistance was limited to electrodes and sample change. Each hole was verified if drilled through. Once drilled, each sample was vibropeen marked.

6.2 Aluminide-coating Process

Machined samples were cleaned in isopropyl alcohol. The next step was the vapor phase aluminizing "above pack" process.

The vapor phase aluminizing (VPA) installation is a full industrial-scale furnace equipped with carbon boxes and plates shown Fig. 10. The donor in the form of a pellet and activator were distributed on the box bottom evenly. Then, a carbon perforated plate was installed as a base for positioning of components to coat.

Fig. 10. *Bell-cover with boxes before loading to VPA furnace*

The sample was installed on a hanger and placed in a box, and then moved under a sealed bell-cover in the aluminizing process. The hangers were previously qualified to ensure coating results like the components.

The protective gas is sent to the boxes and the bell-cover with the appropriate flow rate after whole air evacuation by reaching a high vacuum level. Load temperature and argon flows (primary and secondary) are key controlled parameters. The bell-cover was removed after cooling below 300 ºC. After reaching ambient temperature, carbon boxes were disassembled. The sample was dedicated to lab preparation without further post coating heat treatment in "as coated" condition.

The consumable materials are collected in Table 2 and heat treatment process shown in Table 3 were matched to obtain aluminide coating within aviation industry requirements.

Table 2. *Consumables used in standard aluminization process*

Material	Function	Chemical composition	Quantity
Al-Cr alloy (granulates)	Donor	30/70	50 kg
Ammonium fluoride (powder)	Activator	NH4F	40 kg
Protective gas	Protection	Technical Ar	as needed

Coating is done following dedicated cycle.

Table 3. *Coating heating testament process cycle*

Phase	Set point [ºC]	Main argon flow [l/h]	Secondary argon flow [l/h]	Time /ramp [h]
Heating	800	2500		2.0
Soak	800	2500		0.5
Heating	1050	2500		2.0
Heating	1080	2500		0.5
Soak	1080	2500		6.0
Cooling	300	3600	300	Until set temperature reached

6.3 Oxidation Test

Next, the sample was placed in a high temperature furnace, heated up to 1100 ºC and held in air atmosphere for 23 hours and then cooled down in the furnace. An oxidized plate was cut following the cut-up plan and subsequently a mount was processed. Several grades of sandpaper were used for sample preparation. Final polishing was done with diamond paste.

7 RESULTS

7.1 Diameter and Surface Roughness of Drilled Holes

The first measurement was geometrical holes verification. Each hole was 3D scanned using the Alicona system. Figure 11 shows a scan example. A dedicated macro was used for scanning and geometry extraction automation. That also reduced the operator influence on the measurement. The average diameter for largest holes (A) was: 1.085 mm with standard deviation 0.02 mm, for medium holes (B): 0.639 mm with standard deviation 0.016 mm and the smallest (C): 0.394 mm with standard deviation of 0.009 mm.

One plate was cut, and a hole was opened through polishing to allow hole wall roughness measurement (Fig. 12). The hole internal surface roughness is about 3.2 Ra. This was also done with the Alicona system. At this point, roughness was not a subject of further evaluation.

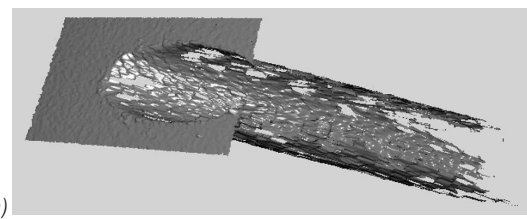

a)

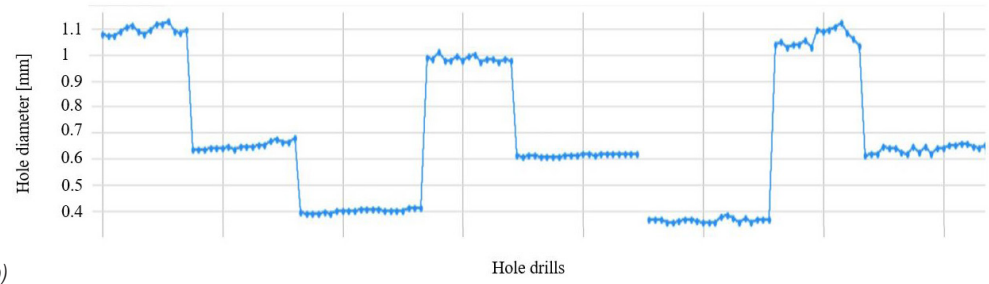

b)

Fig. 11. *a) Scan of the hole, and b) measurements of the pattern*

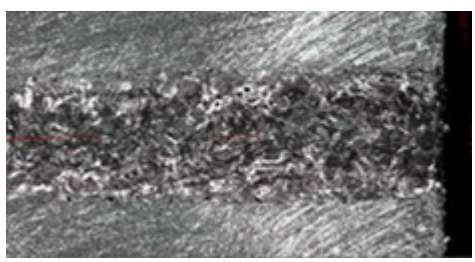

Fig. 12. *Hole side wall view*

7.2 As Drilled Surface Characterization

Prior coating of the "as drilled" sample was evaluated for surface condition. Fig. 13 shows the hole surface. Remelted material is visible. The performed material compositing analysis did not reveal any significant deviation from INCO 718. Moreover, no electrode material was recorded. Composition is shown on Fig. 14.

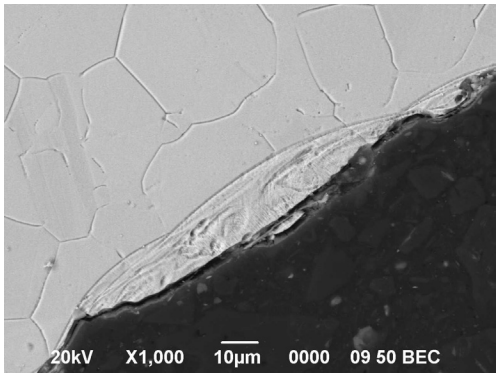

Fig. 13. *View of remelted material (recast)*

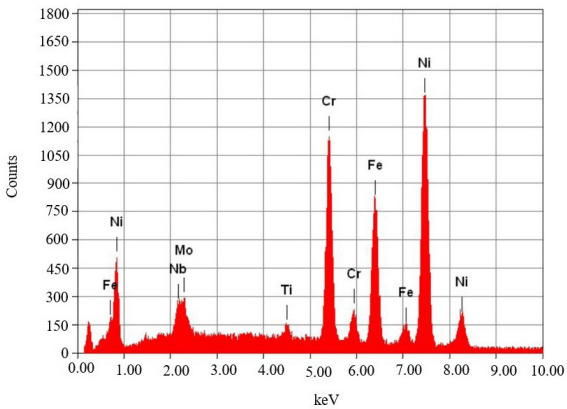

Fig. 14. *Recast composition*

7.3 Coating Characterization

Post-coating metallographic evaluation was performed on one half of the sample. Coating was evaluated for thickness (Fig. 16), inclusions (Fig. 17), and aluminium content. Visual observation of all holes was performed. It was noticed that smaller hole additive coating layer contains more contaminants (dark areas) comparing to other two-hole sizes.

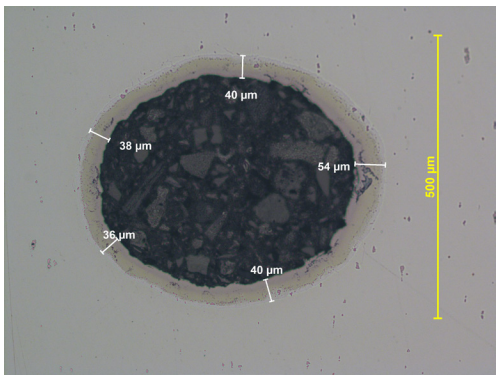

Fig. 15. *Section view of type "A" hole drilled with 0.3 mm electrode*

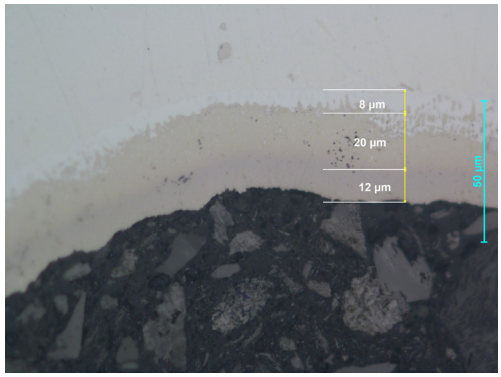

Fig. 16. *Coating thickness for "A" hole. Three layer visible: diffusion, build-up, build-up blue zone*

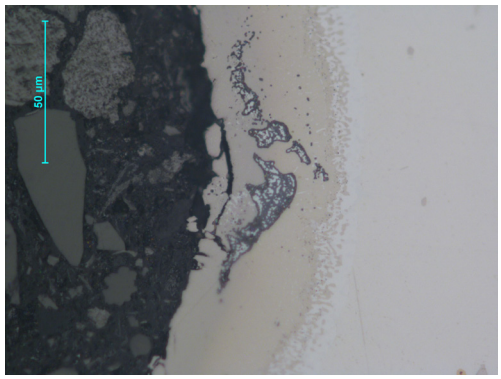

Fig. 17. *Coating inclusion for type "A" hole*

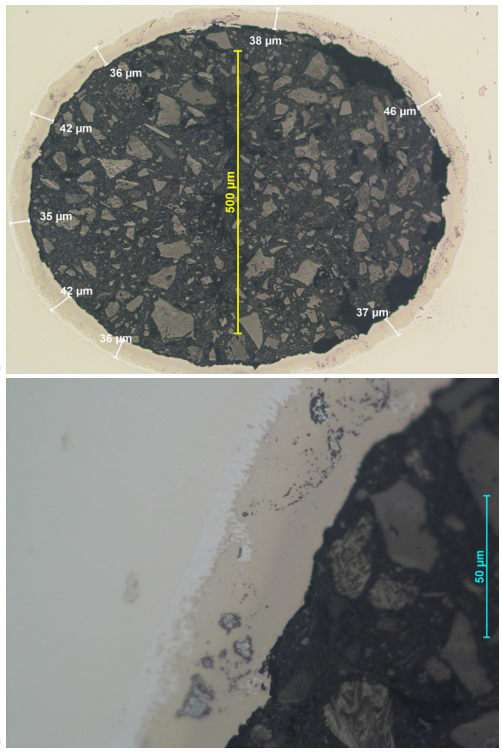

Fig. 18. Section view of type "B" hole drilled with 0.4 mm electrode; a) complete hole view, and b) coating debris

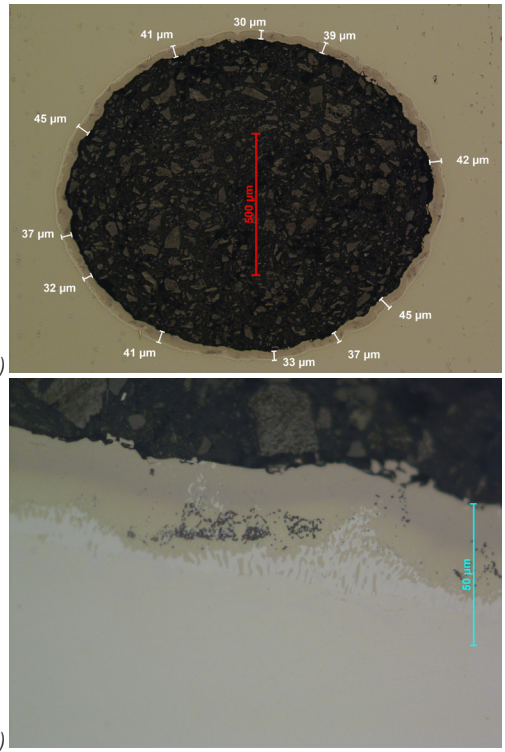

Fig. 19. *a) Section view of the type "C" hole milled with 0.4 electrode, and b) coating inclusions*

During the evaluation, the authors had no apparatus or software to perform quantitative measurements on inclusion quantity or their total area. If studies are continued, such equipment could allow for more precise evaluation. Coating thickness was measured (Figs. 18 and 19). Measurements were made with a Keyence VHX7000 microscope. Fig. 22 shows box plot graph summarizing thickness measurements.

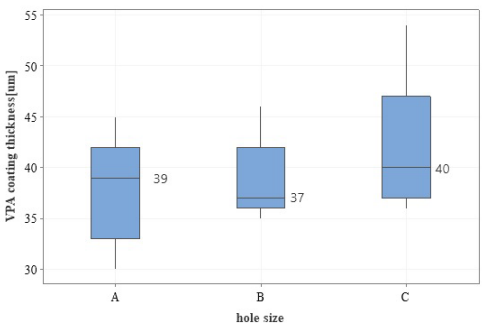

Fig. 20. *Example of coating thickness (overall) measurements for smallest hole and summary box plot*

SEM evaluation revealed that the coating consists of two layers: additive and diffusion. The JEOL JSM-6490LA device was used for measurements. As mentioned, dark areas have also been observed during this evaluation. Similarly, as for visual examination, the smallest hole section is used to show results (Fig. 21a and c).

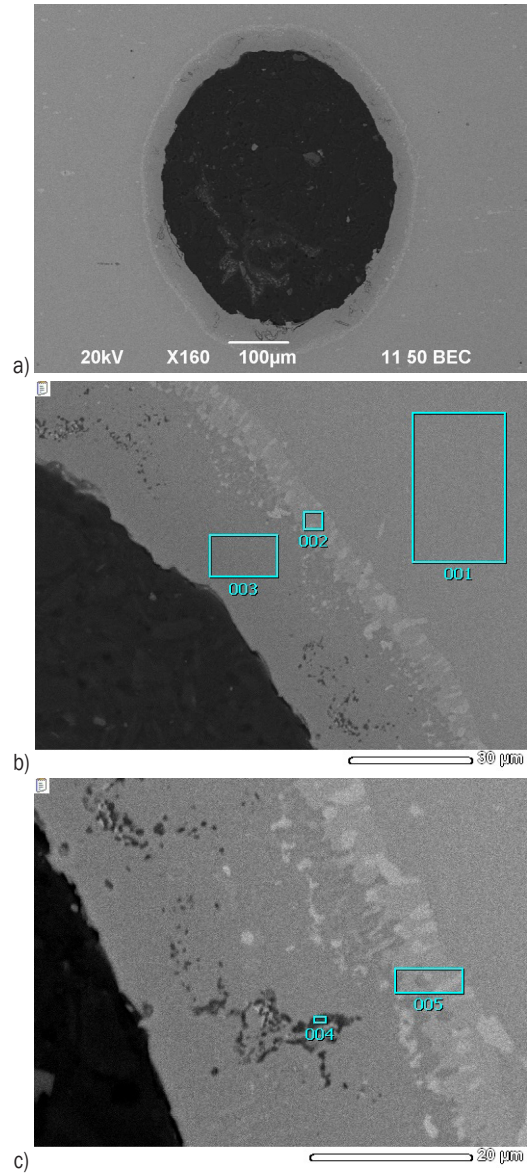

Fig. 21. *a) hole section, and b) and c) EDS zones*

EDS analysis confirmed aluminium content; however, in case of dark spots, oxygen was also detected. It might be assumed that dark spots are alumina oxides. For zones 2 (Fig. 21b) and 5 (Fig. 21c) examination of hole C coating, as well as EDS results show higher aluminium content than alloy composition. Zone 1 (Fig. 21b) shows composition corresponding to Inconel, except for carbon which might come from the resin used for mount preparation.

Table 4. *EDS results for zones 1 to 5*

	EDS zone [mass %]				
Element	1	2	3	4	5
C	1.99	4.38	3.14	10.23	1.6
O				10.79	1.91
Al	0.32	1.7	15.14	29.85	3.39
Ti	0.85	0.56		0.46	0.66
V		0.58			
Cr	17.65	35.69	2.64	5.47	31.43
Mn		1.48			0.88
Fe	19.6	27.9	9.5	7.06	24.76
Ni	54.73	24.63	69.59	30.68	27.35
Nb	3.59				5.39
Mo	1.27	3.09			2.64

7.4 XRD Testing

The sample's external surface was examined for phase composition. X-ray diffractometry was used. Graphs for two angles (1 and 2 degrees) were made. Both showed the same spectra. Therefore, detailed evaluation was performed only for the 2 degrees angle shown on Figs. 22 and 23.

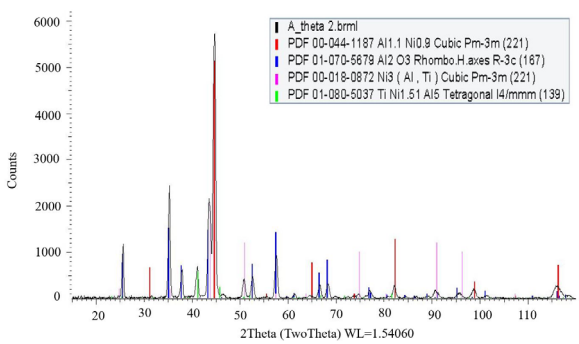

Fig. 22. *Phase analysis for 2deg theta angle*

Surface layer evaluation revealed the presence of aluminide oxide (Al_2O_3) and nickel aluminide (NiAl). This composition was expected and confirmed aluminide type coating existence on the surface.

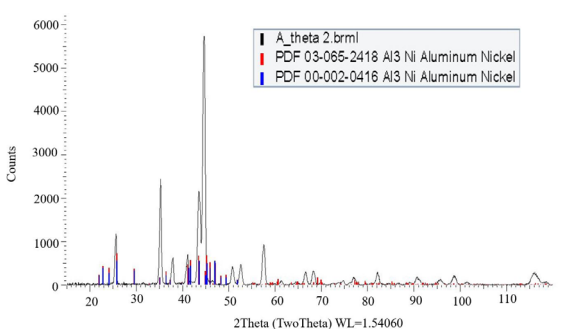

Fig. 23. *Diffractometry with Al3Ni markers on the graph*

Analysis confirmed presence of Al_3Ni, which confirmed the existence of key coating compounds including oxidized aluminium layer.

7.5 Oxidation Testing

Second half of the sample was placed into the air furnace and heated up to 1100 ºC. Atmospheric oxidation test was held for 23 hours. Next, the sample mount was prepared. Visual examination conducted with the Keyence 7000 device revealed a coating thickness reduction, as well as surface degradation. Fig. 24a shows post oxidation SEM examination of hole outline. The zoomed area in Fig. 24b contains alumina rich dark spots.

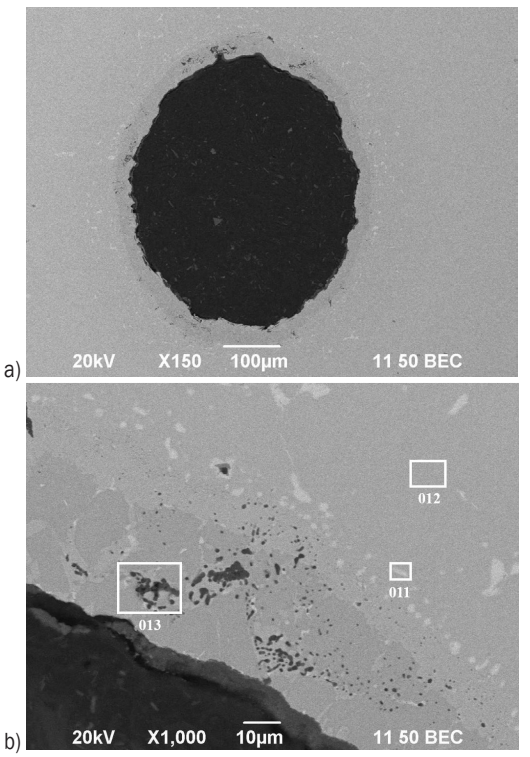

Fig. 24. *a) hole section, and b) EDS zones*

Zone 13 shown on Fig. 24b shows almost 40 % weight of aluminium together with oxygen. Zone 11 is dominated by Nb. Such Nb rich spots were not observed before oxidation testing. It is suspected that heat treatment drove topologically closed pack segregation.

Oxidation testing reduced coating thickness for all hole diameters. However, the most significant reduction was observed for 0.35 mm diameter holes. Coating was reduced by one thirds of its initial thickness. The results shown on Fig. 25 seem to

confirm the hypothesis that EDM process residuals (remelts, oxides) contaminate coating process and by that reduce its durability.

Table 5. *Coating thickness before and after oxidation*

Hole type	Coating thickness after HT [mm]	Coating thickness after oxidation [mm]	Thickness change [%]
A	38	32	18
B	39	30	23
C	42	28	32

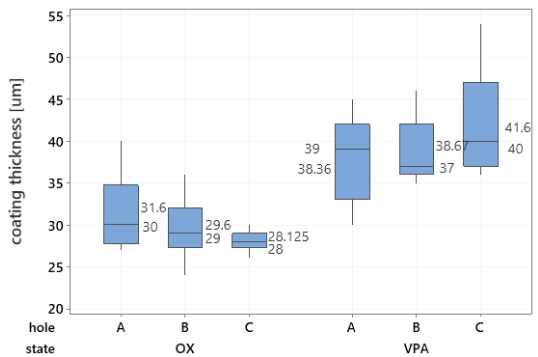

Fig. 25. *Comparison of coating thickness for as coated holes VPA and after oxidation test*

7.6 Scratch Test

The scratch test did not reveal loss of adhesion. Initial results of the test with 100 N final load and 4 mm scratch length, were questioned, and procedure was repeated for several loads (20 N, 40 N, 60 N, 80 N, and 200 N). However, all tests gave same results. A lack of clear coating damage during scratch test. Fig. 26 shows scratch as well as its end close view. The same observation was made by Kukla et al. [29].

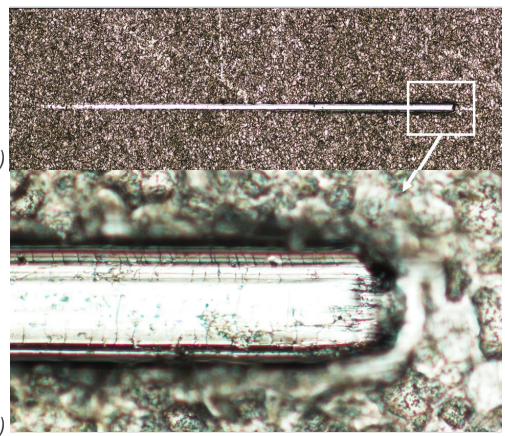

Fig. 26. *Scratch made with load increasing up to 20 N over 4 mm; a) complete scratch, b) zoomed end of scratch visible parent material with cracks introduced by the indenter*

8 CONCLUSIONS

The manufacturing of cooling holes by means of EDM is widely researched. Process parameters, electrode materials, and dielectrics used for the process are being verified by means of advanced statistical tools. More often, traditional mathematical models are replaced by machine learning.

It is shown within this paper that:

a) VPA aluminide coating may be deposited within holes 0.4 mm in diameter;
b) XRD testing proved coating consist of NiAl and Ni_3Al, and Al_2O_3. The last compound provides component corrosion resistance;
c) 1100 ºC 23 h oxidation test resulted in coating thinning from 18 % up to 32 % for smallest holes.

The available literature does not investigate the influence of EDD-modified surfaces on aluminide coating durability. As the test results show, manufacturing process such as EDD has an influence on coating composition and by that on its durability. That hypothesis requires further deeper investigation.

9 FUTURE WORK

The performed evaluation revealed influence of EDD on aluminide coating durability. Future work will focus on:

a) coating durability in deep holes (l/d>> 30),
b) oxidation testing of the VPA and CVD coated holes,
c) improvements in both hole manufacturing methods (improved flushing, di-water additives, electrode modifications) as well as coatings (dopants, thermal cycle changes).

10 ACKNOWLEDGEMENT

Project co-financed by the European Union within the European Regional Development Fund Smart Growth Operation Programme 2014-2020 – Grant Agreement No. POIR.01.01.01-00-D007/16 "Development of cooling technology for hot section components in rotating machines with particular reference to high-pressure turbine blades and vanes.

11 REFERENCES

[1] The Jet Engine (1988). *Rolls-Royce*, London.
[2] Bunker, R.S. (2017). Evolution of turbine cooling. *Proceedings of the ASME Turbo Expo 2017: Turbomachinery Technical Conference and Exposition, vol 1: Aircraft Engine; Fans and Blowers; Marine*, **DOI:10.1115/GT2017-63205**

[3] Tamarin, Y. (2002). *Protective Coatings for Turbine Blades*. ASM International, Materials Park.

[4] Winbro Group Technologies (2022). From: *https://www.winbrogroup.com*, accessed on 2022-04-19.

[5] Bunker, R.S. (2009). The effects of manufacturing tolerances on gas turbine cooling. *ASME Journal of Turbomachinerry*, vol. 131, no. 4, art. ID 041018, **DOI:10.1115/1.3072494**.

[6] Li, Z.Y., Wei, X. T., Guo, Y. B., Sealy, M.P. (2015). State-of-art challenges, and outlook on manufacturing of cooling holes for turbine blades. *Machining Science and Technology*, vol. 19, no. 3, p. 361-399, **DOI:10.1080/10910344.2015.1051543**.

[7] Zielinska, M., Sieniawski, J., Yavorska, M., & Motyka, M. (2011). Influence of chemical composition of nickel based superalloy on the formation of aluminide coating. *Archives of Metallurgy and Materials*, vol. 56, no. 1, art. ID 193, **DOI:10.2478/v10172-011-0023-y**.

[8] Kunieda, M. Lauwers B., Rajurkar K.P., Schumacher, B.M. (2005). Advancing EDM through fundamental insight into the process. *CIRP Annals*, vol. 54, no.2, p. 64-87, **DOI:10.1016/S0007-8506(07)60020-1**.

[9] Machno, M. (2019). Impact of process parameters on the quality of deep holes drilled in inconel 718 using EDD. *Materials*, vol. 12, no. 14, art. ID 2298, **DOI:10.3390/ma12142298**.

[10] Kang, S.H., Kim, D.E. (2006). Fatigue crack susceptibility of electrical discharge drilled holes in nickel based heat resistant alloy. *Materials Science and Technology*, vol. 22, no. 1, p. 21-28, **DOI 10.1179/174328406X78389**.

[11] Novovic, D., Dewes, R.C., Aspinwall, D.K,. Voice, W., Bowen, P. (2004). The effect of machined topography and integrity on fatigue life. *International Journal of Machine Tools & Manufacture*, vol. 44, no. 2-3, p. 125-134, **DOI:10.1016/j.ijmachtools.2003.10.018**.

[12] Ekmekci, B., Sayar, A., Öpöz, T.T., Erden, A. (2009) Geometry and surface damage in micro electrical discharge machining of micro-holes. *Journal of Micromechanics and Microengineering*, vol. 19, no. 10, art. ID 105030, **DOI:10.1088/0960-1317/19/10/105030**.

[13] Sun, W., Xu, Y., Hu, C., Liu, X. (2017) Effect of film-hole configuration on creep rupture behavior of a second generation nickel-based single crystal superalloys. *Materials Characterization*, vol. 130, p. 298-310, **DOI:10.1016/j.matchar.2017.06.019**.

[14] Lazarenko, B.R. (1943). *To Invert the Effect of Wear on Electric Power Contacts*. PhD thesis. The All-Union Institute for Electro Technique, Moscow. (in Russian)

[15] Ramasawmya, H., Blunt, L. (2004). Effect of EDM process parameters on 3D surface topography. *Journal of Materials Processing Technology*, vol. 148, no. 2, p. 155-164, **DOI:10.1016/S0924-0136(03)00652-6**.

[16] Li, C., Li, Y., Tong, H., Zhao, L. (2016). Thinning process of recast layer in hole drilling and trimming by EDM. *Procedia CIRP*, vol. 42, p. 575-579, **DOI:10.1016/j.procir.2016.02.262**.

[17] Świercz, R., Oniszczuk-Świercz, D., Chmielewski, T. (2019). Multi-response optimization of electrical discharge machining using the desirability function. *Micromachines*, vol. 10, no. 1, art. ID 72, **DOI:10.3390/mi10010072**.

[18] Lee, H.T., Tai, T.Y. (2003). Relationship between EDM parameters and surface crack formation. *Journal of Materials Processing Technology*, vol. 142, no. 3, p. 676-683, **DOI:10.1016/S0924-0136(03)00688-5**.

[19] Sarıkaya, M., Yılmaz, V. (2018). Optimization and predictive modeling using S/N, RSM, RA and ANNs for micro-electrical discharge drilling of AISI 304 stainless steel. *Neural Computing & Application*, vol. 30, p. 1503-1517, **DOI:10.1007/s00521-016-2775-9**.

[20] Reed, R.C. (2006). *The Superalloys Fundamentals and Applications*. Cambridge University Press, New York, **DOI:10.1017/CBO9780511541285**.

[21] Ejaz, N., Tauqir, A. (2006). Failure due to structural degradation in turbine blades. *Engineering Failure Analysis*, vol. 13, no. 3, p. 452-463, **DOI:10.1016/j.engfailanal.2004.12.041**.

[22] Zielinska, M., Zagula-Yavorska, M., Sieniawski, J., Filip, R. (2013). Microstructure and oxidation resistance of an aliminide coating on the nickel based supperalloy MAR M247 deposited by the CVD alumionizing process. *Archives of Metallurgy and Materials*, vol. 58, no. 3, p. 697-701, **DOI:10.2478/amm-2013-0057**.

[23] He, J.L., Yu, C.H., Leyland, A., Wilson A.D., Matthews, A. (2002). A comparative study of the cyclic thermal oxidation of PVD nickel aluminide coatings. *Surface and Coatings Technology*, vol. 155, no. 1, p. 67-79, **DOI:10.1016/S0257-8972(02)00025-7**.

[24] Zagula-Yavorska, M., Kocurek, P., Pytel, M., Sieniawski, J. (2016). Oxidation resistance of turbine blades made of ZS6K superalloy after aluminizing by low-activity CVD and VPA methods. *Journal of Materials Engineering and Performance*, vol. 25. p. 1964-1973, **DOI:10.1007/s11665-016-2032-5**.

[25] Zagula-Yavorska, M., Romanowska, J., Pytel, M., Sieniawski, J. (2015). The microstructure and oxidation resistance of the aluminide coatings deposited by the CVD method on pure nickel and hafnium-doped nickel superalloys. *Archives of Civil and Mechanical Engineering*, vol. 15, no. 4, p. 862-872, **DOI:10.1016/j.acme.2015.03.006**.

[26] Zagula-Yavorska, M., Sieniawski, J. (2018). Cyclic oxidation of palladium modified and nonmodified aluminide coatings deposited on nickel base superalloys. *Archives of Civil and Mechanical Engineering*, vol. 18, no. 1, p. 130-139, **DOI:10.1016/j.acme.2017.05.004**.

[27] Wu, Q., Yang, R., Wu, Y., Li, S., Ma, Y., Gong, S. (2011). A comparative study of four modified Al coatings on Ni3Al-based single crystal superalloy. *Progress in Natural Science: Materials International*, vol. 21, no. 6, p. 496-505, **DOI:10.1016/S1002-0071(12)60089-6**.

[28] Cigada, P.A. (2011). *Diffusion Coatings for High- Temperature Applications on Ni-based Superalloys*. Politechnico di Milano, Milan.

[29] Kukla, D., Kopec, D., Kowalewski, Z.L., Politis, D.J., Jozwiak, S., Senderowski, C. (2020) Thermal Barrier Stability and Wear Behavior of CVD Deposited Aluminide Coatings for MAR 247 Nickel Superalloy. *Materials*, vol. 13, no. 17, art. ID 3863, **DOI:10.3390/ma13173863**.